Virology 277, 450–456 (2000)
doi:10.1006/viro.2000.0619, available online at http://www.idealibrary.com on IDEAL®

Mechanism of Capsid Assembly for an Icosahedral Plant Virus

Adam Zlotnick,*[,1] Ryan Aldrich,* Jennifer M. Johnson,* Pablo Ceres,* and Mark J. Young†

*Department of Biochemistry and Molecular Biology, University of Oklahoma Health Sciences Center, Oklahoma City, Oklahoma 73190; and †Department of Plant Sciences, Montana State University–Bozeman, Bozeman, Montana 59717

Received July 25, 2000; returned to author for revision August 21, 2000; accepted August 31, 2000

Capsids of spherical viruses share a common architecture: an icosahedral arrangement of identical proteins. We suggest that there may be a limited number of common assembly mechanisms for such viruses. Previous assembly mechanisms were proposed on the basis of virion structure but were not rigorously tested. Here we apply a rigorous analysis of assembly to cowpea chlorotic mottle virus (CCMV), a typical, small, positive-strand RNA virus. The atomic resolution structure of CCMV revealed an interleaving of subunits around the quasi-sixfold vertices, which suggested that capsid assembly was initiated by a hexamer of dimers (Speir *et al.,* 1995, *Structure* 3, 63–78). However, we find that the capsid protein readily forms pentamers of dimers in solution, based on polymerization kinetics observed by light scattering. Capsid assembly is nucleated by a pentamer, determined from analysis of the extent of assembly by size-exclusion chromatography. Subsequent assembly likely proceeds by the cooperative addition of dimers, leading to the $T = 3$ icosahedral capsid. At high protein concentrations, the concentration-dependent nucleation reaction causes an overabundance of five-dimer nuclei that can be identified by classical light scattering. In turn these associate to form incomplete capsids and pseudo-$T = 2$ capsids, assembled by oligomerization of 12 pentamers of dimers. The experimentally derived assembly mechanisms of $T = 3$ and pseudo-$T = 2$ CCMV capsids are directly relevant to interpreting the structure and assembly of other $T = 3$ viruses such as Norwalk virus and pseudo-$T = 2$ viruses such as the vp3 core of blue tongue virus.

Key Words: capsid assembly; virus assembly; bromovirus; cowpea chlorotic mottle virus; protein polymerization; protein folding.

INTRODUCTION

The assembly of spherical (or icosahedral) viruses remains a poorly understood process, in which many subunits must polymerize rapidly and with high fidelity to form the virus capsid. About half the known virus families have capsids that are arranged with icosahedral geometry. Icosahedral capsids are constructed of 60T subunits (where T is an integer) (Caspar and Klug, 1962); assembly cannot occur by a single high-order reaction. Assembly reactions probably require a cascade of low-order steps and may be further complicated by nucleation, cooperativity, and binding to the viral genome. Because of the simple geometric architecture, it is attractive to postulate that there are a relatively small number of assembly mechanisms for icosahedral capsids. We have recently developed a simple mathematical model of capsid assembly that allows for the analysis of assembly kinetics (Zlotnick *et al.,* 1999). In this report we study the assembly of empty cowpea chlorotic mottle virus (CCMV) capsids. We take advantage of this *in vitro* system to examine protein–protein interaction without the complication of protein–RNA interactions. Understanding assembly of empty capsids will help identify the role that the capsid protein plays in directing virus assembly, providing insight into the virus life cycle and mechanisms to disrupt the virus assembly for therapeutic or biotechnology applications.

The bromoviruses, in particular CCMV, provide an attractive model system for examining icosahedral virus assembly. Bromoviruses are members of the Bromoviridae virus family (alphavirus-like superfamily). The 28-nm icosahedral virus particles encapsidate four positive-sense, single-stranded viral RNAs (for reviews see Bancroft and Horne, 1977; Lane, 1981; Ahlquist, 1992). The RNA genome is packaged into three virus particles, all with similar or identical capsid structures (Fox *et al.,* 1998). RNA 1 and RNA 2, which encode proteins involved in RNA-dependent replication, are each packaged in separate particles. RNA 3 (an mRNA encoding 32-kDa viral movement protein) and RNA 4 (a subgenomic RNA derived from RNA 3, which serves as an mRNA for the 20-kDa coat protein) are copackaged into a third particle in a 1:1 molar ratio (Loesch-Fries and Hall, 1980). All three virions are required to establish infection of plants. Virus particles purified from infected plant cells contain only viral RNAs.

CCMV has been used as a model system for viral

[1] To whom correspondence and reprint requests should be addressed at University of Oklahoma Health Sciences Center, Department of Biochemistry and Molecular Biology, P.O. Box 26901, BRC464, Oklahoma City, OK 73190. Fax: (405) 271-3910. E-mail: adam-zlotnick@ouhsc.edu.

0042-6822/00 $35.00

assembly since Bancroft and Hiebert first demonstrated that purified RNA and coat protein can reassemble *in vitro* to produce infectious virions (Bancroft and Hiebert, 1967; Hiebert *et al.,* 1968; Bancroft *et al.,* 1968, 1969; Hiebert and Bancroft, 1969). One unique aspect of the CCMV *in vitro* assembly/disassembly system is that a wide range of polymorphic forms of the virion assembles in varied chemical environments (Bancroft and Hiebert, 1967; Hiebert *et al.,* 1968; Bancroft *et al.,* 1968, 1969; Hiebert and Bancroft, 1969; Speir *et al.,* 1995). This suggests that changes in ionic strength, pH, and temperature can affect both the protein–protein and protein–RNA interactions in virion assembly and disassembly.

CCMV capsid protein can be isolated as a stable 40-kDa homodimer at neutral pH (Adolph and Butler, 1974). Decreasing the pH at high ionic strength (pH 5.5 and I = 0.5, respectively) causes coat protein dimers to form empty capsids (Bancroft *et al.,* 1968). Formation of empty capsids is strictly an *in vitro* effect. Empty particles have not been observed in natural infections. This property provides a novel system for distinguishing the roles protein–protein and protein–RNA interactions contribute to virus assembly and structure. The structure of the empty capsids is indistinguishable from that of RNA-containing virus particles (Fox *et al.,* 1998).

The structure of CCMV has been determined to 3.3-Å resolution by X-ray crystallography (Speir *et al.,* 1995) and exhibits several features not seen in other plant viruses. The quaternary structure of CCMV displays a $T = 3$, quasi-symmetry with 32 prominent pentameric and hexameric capsomers. Each coat protein subunit is comprised of an eight-stranded, antiparallel, β-barrel core that is similar to the fold found in the capsid proteins of many other spherical plant and animal viruses (Rossmann and Johnson, 1989; Harrison, 1990; Johnson and Speir, 1997); the capsomers are formed from these β barrels. Extending in opposite directions away from the β-barrel core are the C-terminal and N-terminal arms of the coat protein. The pentameric and hexameric capsomers of the virion are linked through C-terminal extensions originating from two coat proteins. This linkage stabilizes the noncovalent dimer. The C-terminal extension from one coat protein subunit extends across twofold or quasi-twofold axis and invades the adjacent coat protein subunit. The N-terminal arm from the adjacent subunit "clamps" the invading C-terminal arm. In addition to providing the clamp, the N-terminal extensions of the threefold related coat proteins converge at the quasi-sixfold vertices of the virion and intertwine to form a hexameric tubular structure (β-hexamer) beneath the contiguous protein shell. The presence of the β-hexamer suggests that it plays a principal stabilizing factor in the virion (Speir *et al.,* 1995; Zhao *et al.,* 1995). Five N-terminal arms also extend toward each icosahedral fivefold axis, but they do not form a similar structure. The N- and C-terminal extensions provide an intricate network of "ropes" that "tie" subunits together.

A general model for CCMV assembly was proposed based on the CCMV high-resolution structure and previously reported biochemical observation of assembly *in vitro* (Speir *et al.,* 1995). The model proposed that the noncovalent coat protein dimer was the basic assembly unit. The noncovalent dimer was postulated to form into a hexamer of dimers that is stabilized by the β-hexamer. Subsequent addition of noncovalent dimers, viral RNA, and divalent cations to the hexamer of dimers resulted in the formation of the $T = 3$ icosahedral particle.

Recently, we began to rigorously address the physical mechanism and regulation of virus assembly (Zlotnick, 1994; Zlotnick *et al.,* 1999). We approached the problem of capsid assembly by describing the assembly process as a cascade of low-order reactions, including the possibility of a nucleating step. Theory predicts that reaction kinetics will be sigmoidal, with an infinitesimal concentration of intermediates at equilibrium; intermediates may accumulate transiently. Based on the theoretical treatment, we developed simple tools that allow us to estimate the size of a nucleating species and the order of subsequent elongation reactions (Zlotnick *et al.,* 1999). We now apply these tools to CCMV.

RESULTS

Polymerization kinetics have multiple phases

We find that CCMV capsid assembly kinetics are both pH and concentration dependent, in agreement with earlier equilibrium observations (Bancroft and Hiebert, 1967; Adolph and Butler, 1976). Based on theory and the example of hepatitis B virus (Zlotnick *et al.,* 1999), we expected to see sigmoidal kinetics, with a lag phase followed by rapid assembly. However, we observed multiphase assembly kinetics (Fig. 1A, inset). CCMV assembly reactions initially had a rapid increase in light scatter that leveled off. Superimposed on this first phase was a second phase of increasing light scatter. We hypothesized that this behavior resulted from rapid formation of oligomers followed by slow formation of capsids. The initial assembly reaction products may be part of the normal capsid assembly path. This hypothesis leads to the prediction that, when there is a great abundance of this early polymerization product, capsid assembly may start from so many "nuclei" that the reaction will yield more incomplete or aberrant particles. Counterintuitively, slower assembly would lead to more capsids. The concentration of capsids assembled and the kinetics of their appearance, determined by chromatography (see below), are consistent with these predictions.

The first phase of capsid protein polymerization had fifth-power concentration dependence in pH 5.25 assembly buffer (Figs. 1B and 1C). We extracted the power dependence of this phase from the log of the rate of light

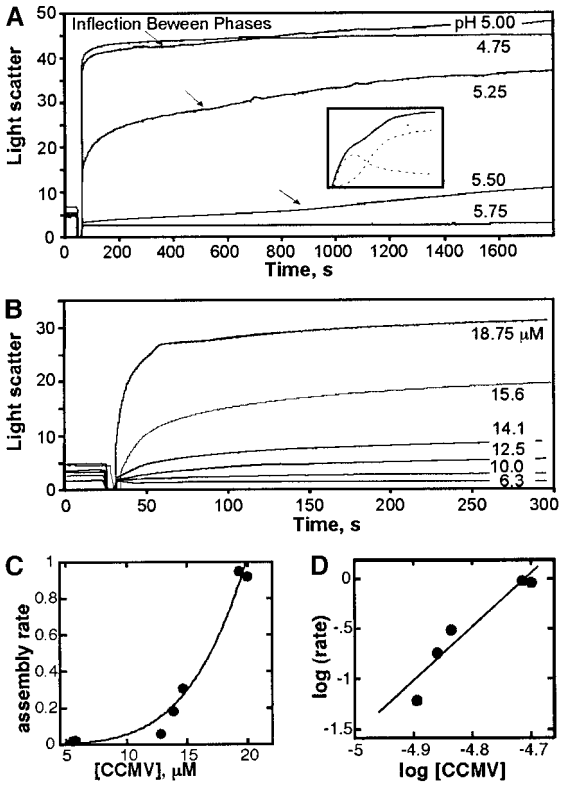

FIG. 1. CCMV capsid protein assembly observed by light scattering. (A) Assembly of 10-μM capsid protein is pH dependent. Light scatter is measured in arbitrary units. Very fast assembly at pH 4.75 resulted in formation of kinetically trapped intermediates and attenuation of light scatter. At long times, evidence for two concurrent reactions was evident, which was interpreted as rapid oligomer formation and slow capsid formation, shown qualitatively in the inset. The inset is based on the first 600 s of a pH 5.25 assembly of 15 μM protein. The sigmoidal curve for capsid assembly is based on a theoretical model (Zlotnick, 1994; Zlotnick *et al.,* 1999): light scatter for the fast phase is the difference between observed and scatter attributable to capsid. Arrows identify inflection points between the two reactions, which occur near the end of the lag phase preceding capsid assembly. (B) pH 5.25 assembly is concentration dependent. Only the first 300 s, the fast (oligomerization) phase of capsid protein polymerization, is shown. (C, D) The order of the fast phase of the pH 5.25 reaction was derived from the concentration dependence of the rate. The least-squares fit of rate versus [subunit] showed a 4.3-power dependence in a linear-linear plot; a log-log plot fit a 5.5-power law, because the data are weighted differently.

scatter change, at very early times (<20 s), compared to the log of protein concentration (a standard method of determining reaction order). The observed fifth-power concentration dependence suggests that CCMV capsid protein forms pentamers in the first phase of the assembly reaction; these may have an important role in subsequent assembly reactions. In this analysis we assumed that the first phase is homogeneous, with minimal contamination from the second phase. This assumption is supported by our observation that capsids accumulate slowly, even after 300 s (see Fig. 2A). This is the first of several examples of fifth-power concentration dependence observed in independent analyses of CCMV assembly.

Polymerization of capsid protein was both concentration and pH dependent. No polymerization was observed at pH $\geq$ 5.75 for up to 30 μM protein (Fig. 1A). The rate of assembly was greater at lower pH. At pH 5.25, the amplitude of the second phase was greatest compared to the amplitude of the first phase, suggesting efficient capsid formation. At pH 4.75, although the rate of increase of light scatter was fast, the maximum light scattering was attenuated. The attenuated light scattering is attributable to formation of kinetic traps, which were predicted by theory (Zlotnick *et al.,* 1999) and were confirmed by electron microscopy (see Fig. 3).

Assembly kinetics affect the morphology of the reaction products

Negative-stained electron micrographs of assembly reactions support these interpretations: fast assembly can result in kinetic traps and aberrant assembly products. A pH 5.25 assembly reaction with 10 μM CCMV dimer yields a nearly homogeneous population of particles with a diameter of about 280 Å, as expected for $T = 3$ capsids (Fig. 3A). There were very few damaged particles and a small population of smaller particles, approximately 230 Å in diameter. Micrographs of reactions with high protein concentrations, >20 μM dimer, had higher yields of smaller particles (not shown). Assembly at pH 4.75 could mimic the effect of high-concentration assembly at pH 5.25, except that the higher association energy would be expected to yield a larger proportion of kinetically trapped protein (Zlotnick *et al.,* 1999). This is the result that we observed with a 10 μM dimer assembly reaction at pH 4.75 (Fig. 3B), in which the majority of intact capsids were 230 Å in diameter with a high proportion (~30%) of misassembled and partially assembled particles.

Identification of nucleus size, intermediates, and reaction products

Previous analysis of simulations of assembly show that the concentration dependence on the extent of capsid assembly is proportional to the number of subunits in the nucleating species (Zlotnick *et al.,* 1999). It was not possible to evaluate the extent of assembly by light scattering because of the multiple phases and heterogeneous reaction mixture (Fig. 1A). Instead, capsid and dimer concentrations were quantified by liquid chromatography (Fig. 2A). At $t = 300$ s, assembly reactions (pH 5.25) were injected onto a Superose-6 column equilibrated with pH 5.25 assembly buffer. Capsids eluted at 10 ml and dimers eluted at 17 ml. At low capsid protein concentrations (<10 μM), a fifth-power dependence was observed (Figs. 2B and 2C). Fitting a high-order concentration dependence has obvious difficulties (Figs. 2B and

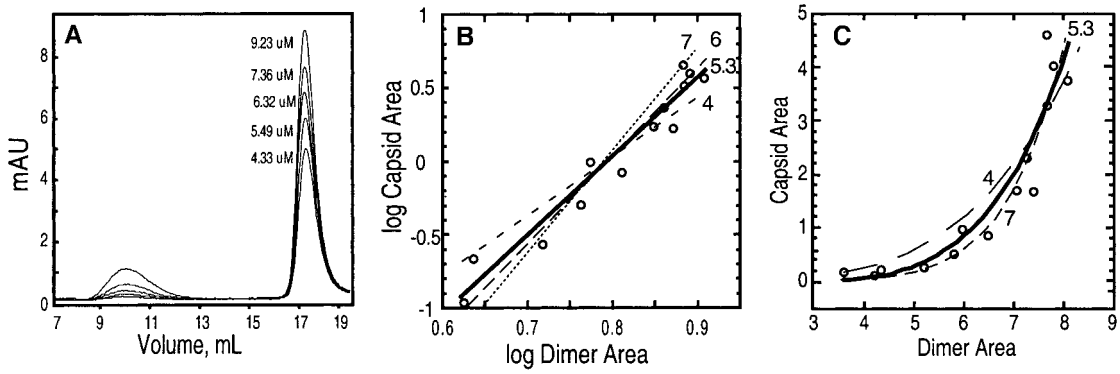

FIG. 2. Concentration dependence of the extent of CCMV capsid assembly was determined using size-exclusion chromatography. (A) Assembly reactions (see Fig. 1) were injected onto a Superose-6 column 300 s after mixing. Elution was monitored at 280 nm. (B, C) Theoretical assembly models (Golmohammadi *et al.,* 1993) predict that the concentration dependence of assembly n, for [capsid] = [free dimer]^n, indicates the size of the nucleating species. We observe a best-fit 5.3-power concentration dependence (heavy line). Concentration dependence was determined in linear-linear and log-log plots with correlation coefficients of 0.93 (B) and 0.97 (C). For comparison, curves constrained to a fourth-, sixth-, or seventh-power concentration dependence are also shown [the sixth-power curve is omitted from (C) for clarity].

2C), where the 5.3- and sixth-power curves are nearly superimposable. However, (1) the data together support a fifth-power assignment (see Discussion) and (2) recent model calculations indicate that nucleus size based on concentration dependence can be slightly overestimated (by <1) in reactions that are susceptible to kinetic traps (Endres and Zlotnick, unpublished observations). Chromatography of reactions at moderate concentrations ($\sim$10–25 μM) revealed a shoulder on the trailing edge of the capsid peak (Figs. 2A and 4A). The shoulder indicates that there was a large population of intermediate species under these conditions. At high concentrations, $T = 3$ capsids were no longer the only reaction product (see Fig. 4B). Assembly kinetics at high concentrations (50 μM) at pH 5.25 resembles the kinetics of pH 4.75 assembly at 10 μM (Figs. 1A and 3B).

Analysis of chromatograms was extended by using a multiangle light-scattering detector and calculating molecular weights using Debye analysis (Fig. 4). Reaction mixtures, at 300 s, were resolved using a Superose-6

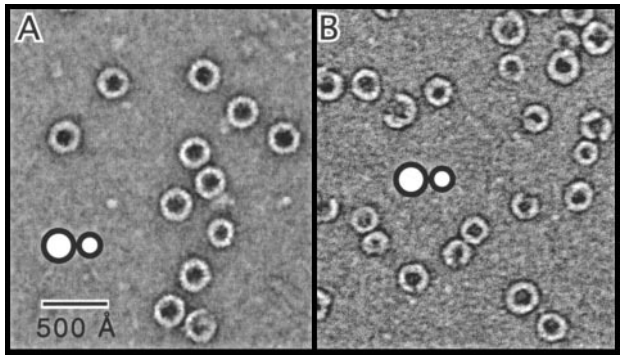

FIG. 3. Negative stain electron microscopy of *in vitro* assembled virus-like particles, from (A) pH 5.25 or (B) pH 4.75 assembly reactions. (A) At pH 5.25, most particles were approximately 280 Å in diameter, with a small population of smaller particles. (B) At pH 4.75, most intact particles were approximately 230 Å in diameter and there was a large population of partial particles. For scale we show a 500-Å bar and circles with diameters of 280 and 230 Å, corresponding to $T = 3$ and pseudo-$T = 2$ particles, respectively.

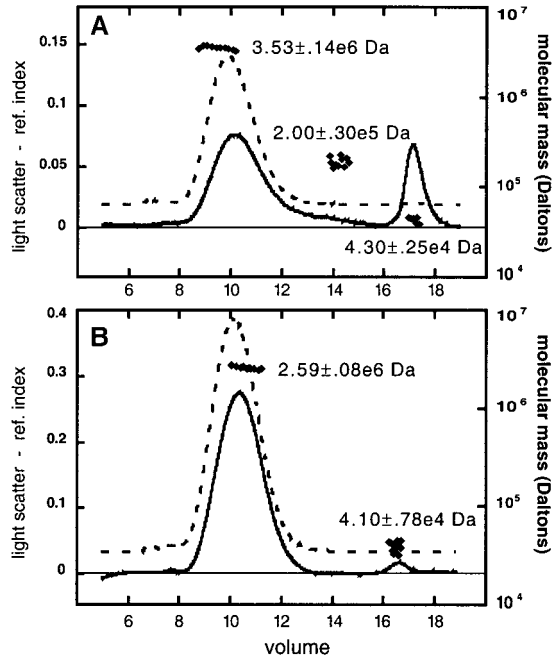

FIG. 4. Analysis of capsid assembly by light-scattering and size-exclusion chromatography shows how protein concentration affects assembly products. (A) For 22-μM capsid protein, major assembly products were 3.5-MDa $T = 3$ capsid and 43-kDa dimer. The right edge of the capsid peak was polydisperse and trailed off to a 200-kDa species (i.e., a pentamer of dimers). (B) Assembly of 53-μM capsid protein yielded peaks with estimated molecular weights of 2.6 MDa and 41 kDa. The capsid peak was shifted 0.4 ml compared to a $T = 3$ capsid. No intermediate species were observed. Chromatographs show the refractive index (solid line), 90° light scattering (dashed line), and molecular weight estimated from Debye plots (diamonds). The molecular weight is estimated for 10-μl slices throughout the chromatograph. The light-scattering curve is offset from the baseline; three-fourths of the molecular mass points are removed for clarity.

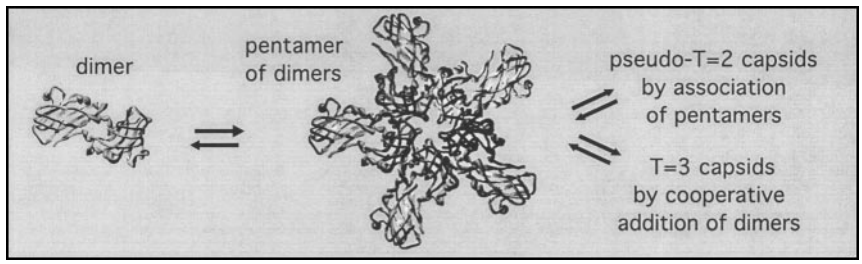

FIG. 5. Scheme describing *in vitro* assembly of CCMV. Assembly of capsid protein begins with formation of a pentamer of dimers. From this starting point, assembly may proceed by cooperative addition of dimers to yield $T = 3$ capsids or by association of pentamers to form pseudo-$T = 2$ particles. Oligomers of CCMV coordinates (Speir *et al.,* 1995) were generated by VIPER (http://mmtsb.scripps.edu/viper/viper.html) and displayed using WEBVIEWER Lite.

column. The main capsid and dimer peaks of a pH 5.25 assembly reaction with 22-μM dimer were largely monodisperse and had estimated molecular weights of 3.5 MDa and 43 kDa, in excellent agreement with the expected values of 3.6 MDa for $T = 3$ capsid and 40 kDa for dimer, respectively (Fig. 4A). We did not observe any 20-kDa capsid protein monomer. The trailing edge of the capsid peak had a noticeable shoulder. It is not known whether the mixture of oligomers at the trailing edge of the capsid peak is the result of dissociation of capsids and partially assembled capsids, or represents a pool of intermediates that are trapped by the separation process. The trailing edge of the shoulder had a calculated molecular weight of 200,000 kDa, a value that is consistent with a pentamer of 40-kDa dimers.

Assembly at higher concentration proceeds faster (Fig. 1B) and also yields aberrant products (Fig. 3B). This was noted in chromatographs in which the capsid peak is shifted slightly to the right, i.e., to smaller Stokes radii (Fig. 4B). Multiangle light-scattering analysis indicated that the average molecular weight of the largely monodisperse peak was about 2.6 MDa. Similarly, when products of a pH 4.75 assembly reaction were resolved by size-exclusion chromatography, the capsid peak was also shifted to the right from the expected elution volume (not shown). Electron micrographs of pH 4.75 assembly reactions had a high proportion of 230-Å-diameter particles, smaller than a $T = 3$ capsid (Fig. 3B). The size (Fig. 3B) and weight (Fig. 4B) of the small complete capsids are consistent with a 2.4-MDa particle constructed from 60 dimers, i.e., a pseudo-$T = 2$ capsid.

DISCUSSION

We have demonstrated that *in vitro* assembly of virus capsids can be observed in real time and interpreted using a simple generalizable analysis. This experimental approach to understanding capsid assembly can be applied to any *in vitro* capsid assembly system.

A simple model of CCMV capsid assembly can be derived from our data (Fig. 5). Dimeric capsid protein readily forms pentamers of dimers, indicated by the fifth-power dependence of the initial assembly phase. These pentamers can serve to nucleate assembly of $T = 3$ capsids, indicated by the fifth-power dependence of the extent of assembly. Based on the structure of the $T = 3$ particle (Speir *et al.,* 1995) and the structural limitations of the pseudo-$T = 2$ particle (Krol *et al.,* 1999), the most likely quaternary structure for the pentamer is a fivefold vertex. We hypothesize that assembly then proceeds by cooperative addition of dimeric subunits to this nucleus, forming pentameric and hexameric capsomeres. This mechanism takes advantage of structural features (e.g., the β-hexamer) observed by crystallography (Speir *et al.,* 1995) and the fast-forming pentamer described here. Typical sites on a growing capsid would require the addition of only two to four subunits at a time. This model successfully explains efficient assembly at low protein concentrations and the accumulation of pentamers at moderate to high concentrations. At the higher concentrations, formation of pentamers depletes the free subunit concentration and impedes assembly, leading to a high yield of partial capsids. At high concentrations, so many pentamers are formed that they associate to yield pseudo-$T = 2$ particles. Only a fivefold pentamer of dimers is consistent with the structure of the pseudo-$T = 2$ capsid (Krol *et al.,* 1999). There are alternatives to this model. For example, preformed pentamers could add to the growing $T = 3$ capsid, but this seems less likely, given that the fraction of aberrant particles increases at higher initial dimer concentrations or lower pH.

Two general theoretical limiting cases have been proposed to describe capsid assembly that can be applied to CCMV assembly, in particular: (1) assembly as a reaction with rapid equilibration between intermediates (EQ) and (2) assembly as unidirectional, kinetically limited reaction (KL) (Zlotnick, 1994; Zlotnick *et al.,* 1999). EQ assembly is characterized by the requirement for weak association energy, the transient presence of a high concentration of intermediates during assembly, and a tendency to form kinetic traps. KL assembly has no limits on association energy or accumulation of intermediates but does require a distinct initiating step, such as nucle-

ation. Under the conditions used in this study, CCMV forms labile capsids, has an appreciable concentration of intermediates during assembly, and is susceptible to kinetic traps. CCMV most closely conforms to the description of EQ assembly. CCMV assembly is nucleated, although nucleation is not precluded by the EQ model. A prediction of the EQ model is that subunits of assembled viruses and virus-like particles should be in equilibrium with free subunits. Evidence for equilibration has been observed with brome mosaic virus, the type member of the bromovirus family, in which capsid protein could be dissociated from RNA1 by exposure to exogenous RNA (Duggal and Hall, 1993). Quantitative CCMV assembly *in vitro* is best accomplished by slowly decreasing the pH of the buffer by dialysis (Zhao *et al.,* 1995), which allows high association energy at the end point and avoids the kinetic traps induced by the rapid assembly protocols used in this study.

At pH 5.25 and high protein concentration, we form high yields of pseudo-$T = 2$ capsids in the absence of RNA (Fig. 4B). The formation of pseudo-$T = 2$ particles is not unique to CCMV. Yeast-expressed brome mosaic virus assembles to form pseudo-$T = 2$ capsids that surround 1200-nucleotide RNA fragments (Krol *et al.,* 1999). The authors concluded that the capsid size was regulated by the amount of encapsidated RNA. The observation of these aberrant particles emphasizes the role of pentamer formation in capsid assembly under physiological conditions. The mechanism(s) of capsid formation with nucleic acid-filled particles is now under investigation.

The structure of CCMV revealed the presence of the novel β-hexamer, an intertwining of N-termini at the quasi-sixfold vertex (Speir *et al.,* 1995). Under some conditions (low ionic strength and low pH), CCMV capsid protein can form sheets and tubes, structures that are constructed entirely of hexamers (Bancroft and Hiebert, 1967; Hiebert *et al.,* 1968; Bancroft *et al.,* 1968, 1969; Hiebert and Bancroft, 1969; Speir *et al.,* 1995). We suggest that the nucleus of the assembly reaction is an important determinant of the subsequent product. For geometric reasons, the pentameric nucleus cannot be incorporated into a sheet, though it is required for the $T = 3$ or pseudo-$T = 2$ icosahedra. By initiating assembly with a pentamer, addition of further subunits necessarily leads to formation of a curved surface; in the case of CCMV this surface closes to form the icosahedral capsid. In general, it is attractive to speculate that assembly, for larger icosahedra or more complicated structures, is nucleated by oligomers that direct the geometry and radius of curvature of the mature capsid. It is also apparent that the nucleus is not always obvious from the structure; the hexamer is the building block of sheets and tubes but is not the nucleus for capsid assembly. It is important to note that the pentamer, which nucleates $T = 3$ capsid assembly *in vitro* and is required for assembly of pseudo-$T = 2$ capsids in yeast (Krol *et al.,* 1999) and *in vitro,* may not be the nucleus for assembly of RNA-filled capsids.

Nonetheless, because of the fivefold symmetry inherent in icosahedral geometry, pentamer formation is likely to be a common regulatory feature in the assembly of many small viruses. Based on structural features, it was speculated that assembly of bacteriophage MS2 (Golmohammadi *et al.,* 1993) and Norwalk virus (Prasad *et al.,* 1999) are initiated by pentamer formation. The proposed assembly paths are essentially the same as the assembly path that we demonstrate for $T = 3$ CCMV. The pseudo-$T = 2$ vp3 shell of blue tongue virus is composed of 120 identical subunits. Again, based on structural considerations, Grimes *et al.* (1998) proposed that fivefold decamers preassembled and then associated to form the capsid. This assembly path closely resembles the path that we propose for pseudo-$T = 2$ CCMV particles. Though observed features may suggest an assembly model, with this study we demonstrate a means for rigorously determining elements of the assembly path that can be experimentally verified.

MATERIALS AND METHODS

Preparation of protein

CCMV capsids were isolated from infected cowpeas and dissociated as previously described (Zhao *et al.,* 1995), except that pefabloc SC (Boerhinger-Mannheim, Indianapolis, IN) was used instead of phenylmethylsulfonyl fluoride. Capsid protein dimers were separated from any remaining RNA by size-exclusion chromatography through a 2.6 × 70-cm Sephacryl S300 column (Amersham-Pharmacia, Piscataway, NJ), equilibrated with dimer storage buffer (20 mM Tris–HCl, pH 7.5, 1 M NaCl, 1 mM DTT). Capsid protein was quantified by absorbance at 280 nm using an extinction coefficient of 36,400 M^{-1} cm^{-1} per dimer.

Light-scattering measurement

Kinetics of capsid protein polymerization were observed by following changes in light scattering using a Spex Fluoromax-2 fluorometer (Instruments SA; Edison, NJ) with emission and excitation monochromators set to 320 nm with a 3-nm bandpass. All experiments were performed using black-masked 50-μl fluorescence microcuvettes (Hellma, Forest Hills, NY). Initial light scatter was observed for 55 μl of dimer in storage buffer for 40 s. At 50 s, 55 μl of assembly buffer at the stated pH (200 mM sodium citrate, 1 M NaCl) was added. All reactions were at room temperature.

Analytical chromatography

Chromatographic quantification of dimer and capsid was performed with an AKTA-FPLC system, using a Su-

perose-6 10/30 column (both from Amersham Pharmacia Biotech, Piscataway, NJ). Reactions were initiated when equal volumes of sample and assembly buffer (100 mM sodium citrate at the desired pH, 1 M NaCl) were mixed. At 300 s, the sample was injected onto the column and eluted at 0.5 ml/min with 0.1 M sodium citrate (pH 5.25), 1 M NaCl, and 1 mM DTT. The elution profiles were quantified and integrated on the basis of absorbance at 280 nm using UNICORN software.

For determination of mass by light scattering, in conjunction with size-exclusion chromatography, the same Superose-6 column was mounted on a Poros HPLC pump and eluted peaks were observed with an Optilab DSP refractometer and a Dawn 18 angle light-scattering detector (both from Wyatt Technology, Santa Barbara, CA). Debye analysis of the eluate was performed at 1-s intervals calculated by the program ASTRA, bundled with the Dawn spectrometer, assuming a *dn*/*dc* difference refractive index of 1.85 for protein.

Electron microscopy

Samples were diluted to <0.1 mg/ml, adsorbed to freshly glow-discharged grids (carbon evaporated over collodian adhered to a 400-mesh copper substrate), and stained with 1% uranyl acetate (all microscopy supplies from EM Science, Fort Washington, PA). Micrographs were recorded on a JEOL 1200EX microscope (JEOL USA, Peabody, MA) retrofitted with an AMT 1K × 1K CCD camera (AMT Electronics, Danvers, MA). A magnification of ×100,000 was used to minimize pixelation of the CCD images.

ACKNOWLEDGMENTS

This research was supported by Research Project Grant RPG-99-339-01 from the American Cancer Society (to A.Z.). R.A. was a participant in the SURE (summer undergraduate research experience) program supported by the Presbyterian Health Foundation. The electron microscope was available through the Oklahoma Medical Research Foundation (OMRF) Imaging Facility.

REFERENCES

Adolph, K. W., and Butler, P. J. G. (1974). Studies on the assembly of a spherical plant virus. I. States of aggregation of the isolated protein. *J. Mol. Biol.* **88,** 327–341.

Adolph, K. W., and Butler, P. J. G. (1976). Assembly of a spherical plant virus. *Philos. Trans. R. Soc. Lond. B Biol. Sci.* **276,** 113–122.

Ahlquist, P. (1992). Bromovirus RNA replication and transcription. *Curr. Opin. Genet. Dev.* **2,** 71–76.

Bancroft, J. B., Bracker, C. E., and Wagner, G. W. (1969). Structures derived from cowpea chlorotic mottle and brome mosaic virus protein. *Virology* **38,** 324–335.

Bancroft, J. B., and Hiebert, E. (1967). Formation of an infectious nucleoprotein from protein and nucleic acid isolated from a small spherical virus. *Virology* **32,** 354–356.

Bancroft, J. B., and Horne, R. W. (1977). Bromovirus (brome mosaic virus) group. *In* "The Atlas of Insect and Plant Viruses" (K. Maramorosch, Ed.). Academic Press, New York.

Bancroft, J. B., Wagner, G. W., and Bracker, C. E. (1968). The self-assembly of a nucleic acid-free pseudo-top component for a small spherical virus. *Virology* **36,** 146–149.

Caspar, D. L. D., and Klug, A. (1962). Physical principles in the construction of regular viruses. *Cold Spring Harb. Symp. Quant. Biol.* **27,** 1–24.

Duggal, R., and Hall, T. C. (1993). Identification of domains in brome mosaic virus RNA-1 and coat protein necessary for specific interaction and encapsidation. *J. Virol.* **67,** 6406–6412.

Fox, J. M., Wang, G., Speir, J. A., Olson, N. H., Johnson, J. E., Baker, T. S., and Young, M. J. (1998). Comparison of the native CCMV virion with *in vitro* assembled CCMV virions by cryoelectron microscopy and image reconstruction. *Virology* **244,** 212–218.

Golmohammadi, R., Valegard, K., Fridborg, K., and Liljas, L. (1993). The refined structure of bacteriophage MS2 at 2.8 Å resolution. *J. Mol. Biol.* **234,** 620–639.

Grimes, J. M., Burroughs, J. N., Gouet, P., Diprose, J. M., Malby, R., Zientara, S., Mertens, P. P., and Stuart, D. I. (1998). The atomic structure of the bluetongue virus core. *Nature* **395,** 470–478.

Harrison, S. C. (1990). Common features in the structures of some icosahedral viruses: A partly historical overview. *Seminars in Virology* **1,** 387–403.

Hiebert, E., and Bancroft, J. B. (1969). Factors affecting the assembly of some spherical viruses. *Virology* **39,** 296–311.

Hiebert, E., Bancroft, J. B., and Bracker, C. E. (1968). The assembly *in vitro* of some small spherical viruses, hybrid viruses, and other nucleoproteins. *Virology* **34,** 492–508.

Johnson, J. E., and Speir, J. A. (1997). Quasi-equivalent viruses: A paradigm for protein assemblies. *J. Mol. Biol.* **269,** 665–675.

Krol, M. A., Olson, N. H., Tate, J., Johnson, J. E., Baker, T. S., and Ahlquist, P. (1999). RNA-controlled polymorphism in the in vivo assembly of 180-subunit and 120-subunit virions from a single capsid protein. *Proc. Natl. Acad. Sci. USA* **96,** 13650–13655.

Lane, L. C. (1981). The bromoviruses. *In* "Handbook of Plant Virus Infection and Comparative Diagnosis" (E. Kurstak, Ed.). Elsevier/North Holland, Amsterdam.

Loesch-Fries, L. S., and Hall, T. C. (1980). Synthesis, accumulation, and encapsidation of individual brome mosaic virus RNA components in barley protoplasts. *J. Gen. Virol.* **47,** 323–332.

Prasad, B. V., Hardy, M. E., Dokland, T., Bella, J., Rossmann, M. G., and Estes, M. K. (1999). X-ray crystallographic structure of the Norwalk virus capsid. *Science* **286,** 287–290.

Rossmann, M. G., and Johnson, J. E. (1989). Icosahedral RNA virus structure. *Annu. Rev. Biochem.* **58,** 533–573.

Speir, J. A., Munshi, S., Wang, G., Baker, T. S., and Johnson, J. E. (1995). Structures of the native and swollen forms of cowpea chlorotic mottle virus determined by X-ray crystallography and cryo-electron microscopy. *Structure* **3,** 63–78.

Zhao, X., Fox, J. M., Olson, N. H., Baker, T. S., and Young, M. J. (1995). In vitro assembly of cowpea chlorotic mottle virus from coat protein expressed in *Escherichia coli* and *in vitro*-transcribed viral cDNA. *Virology* **207,** 486–494.

Zlotnick, A. (1994). To build a virus capsid: An equilibrium model of the self assembly of polyhedral protein complexes. *J. Mol. Biol.* **241,** 59–67.

Zlotnick, A., Johnson, J. M., Wingfield, P. W., Stahl, S. J., and Endres, D. (1999). A theoretical model successfully identifies features of hepatitis B virus capsid assembly. *Biochemistry* **38,** 14644–14652.